Characteristics of Carbon Nanoparticles Synthesized by a Submerged Arc in Alcohols, Alkanes, and Aromatics

Poonlasak Muthakarn,[†,‡] Noriaki Sano,[*,†] Tawatchai Charinpanitkul,[*,‡] Wiwut Tanthapanichakoon,[§] and Tatsuo Kanki[†]

Department of Mechanical and System Engineering, Himeji Institute of Technology, University of Hyogo, 2167 Shosha, Himeji, Hyogo 671-2201, Japan, Center of Excellence in Particle Technology, Department of Chemical Engineering, Chulalongkorn University, Patumwan, Bangkok 10330, Thailand, and National Nanotechnology Center, National Science and Technology Development Agency, Klong Luang, Phathumthani 12120, Thailand

Received: June 3, 2006; In Final Form: July 11, 2006

Fullerene-related carbon nanostructures can be synthesized by an arc-in-liquid system as a cost-effective technique. In this work, we investigated the effects of additional carbon sources from liquid media that were alcohols ($C_mH_{2m+1}OH$, $m = 1-8$), alkanes (C_mH_{2m+2}, $m = 6-7$), and aromatic compounds ($C_6H_6-C_nH_{2n}$, $n = 1-2$) on the product structures and the yield of nanocarbon-rich deposits. It was found that carbon nanoparticles (CNPs) that included multi-walled carbon nanotubes (MW-CNTs) and multi-shelled carbon nanoparticles were produced at high concentrations in the hard deposit at the cathode tip formed by the arc in the alcohols and alkanes, similar to that in a water environment. Importantly, not only graphite electrodes but also these organic compounds played a role of a carbon source to produce CNPs that led to an approximately 8−100 times higher yield than the arc-in-water system. There was a tendency that the increase in alcohol concentration and carbon content in the organic molecules positively affected the yield and production rate of the CNPs. However, the selectivity of MW-CNTs was significantly reduced when aromatic compounds were used. Structural analyses by dynamic light scattering and Raman spectroscopy revealed the dependency of the hydrodynamic particle sizes of CNPs and their crystallinity on the liquid components. For a discussion on the reaction mechanism, optical emission spectra of the arc plasma were analyzed to estimate the arc temperature. In addition, liquid byproducts were analyzed by a UV−vis absorbance spectrometer.

Introduction

Nowadays, varieties of nanostructural carbon particles have been widely studied since fullerenes[1] and multi-walled carbon nanotubes (MW-CNTs)[2] were discovered. Single-walled carbon nanotubes (SW-CNTs)[3], carbon nanohorns,[4] nano-onions,[5] and metal-filled carbon nanocapsules[6] have been obtained from various fabrication techniques, which are laser ablation,[7] thermal pyrolysis of gas species,[8] plasma-enhanced chemical vapor deposition,[9] and arc discharge in reduced-pressure gases.[10−12] In addition to these conventional techniques, the arc-in-liquid method has been realized as one of the cost-effective techniques to produce not only carbon nanoparticles[13−22] but also inorganic fullerenes and polyynes.[24−26] In the arc-in-liquid system with water or liquid nitrogen as liquid media, carbon nanoparticles (CNPs) including MW-CNTs and nano-onions are produced from carbon precursors that are supplied from a graphite electrode as a carbon source. It is also known that the liquid that accommodates the arc plasma plays a role of quenching media to cool the carbon precursors in the gas bubbles, resulting in the formation of carbon nanoparticles. Previously, some important parameters of this method have been investigated, such as gas pressure,[15] current density,[18] and liquid flow.[22] However, effects of gas components in bubbles emerging by the arc plasma have not been clarified, although this issue is also a critical factor to determine the characteristics of the products. It is notable that one possible way to increase carbon precursors in the gas bubbles is to provide an additional carbon source into the arc discharge system. Such modification is expected to enable the scale-up production of CNPs because it may solve the problem that CNP production is normally limited by the evaporation rate of graphite electrodes as found in the conventional arc-in-water system. With this concept, liquid components consisting of carbon atoms in their molecules, such as alcohols ($C_mH_{2m+1}OH$, $m = 1-8$), alkanes (C_mH_{2m+2}, $m = 6-7$), and aromatic compounds ($C_6H_{6-}C_nH_{2n}$, $n = 1-2$), are employed as liquid media in the present work with an aim to investigate the effects of liquid components on the structures and selectivity of the CNPs.

Experimental Procedures

The apparatus used in this study is described in a previous paper.[27] A direct current (DC) welding power supply (IKURA ARC, IS-160D) was used to generate arc plasma. Pure graphite rods (99.999%, ToyoTanso) with diameters of 6 and 20 mm were used, respectively, as a movable anode and a cathode. These electrodes were aligned in a vertical direction in 300 mL of liquid, which was placed in a Pyrex glass flask with continuous purge with N_2 to prevent explosion during arcing. The gap between the electrodes was adjusted to be approximately 1 mm to maintain a discharge current of 50 A and a voltage of 20−25 V.

* Corresponding authors. (N.S.) Tel. and fax: +81-792-67-4845; e-mail: sano@eng.u-hyogo.ac.jp. (T.C.) Tel. and fax: +66-2218-6894; e-mail: ctawat@chula.ac.th.

† University of Hyogo.

‡ Chulalongkorn University.

§ National Science and Technology Development Agency.

10.1021/jp063443j CCC: $33.50
Published on Web 08/30/2006

TABLE 1: Arc Stability and Color of Residual Liquid after Arc Discharge in Two Solutions (CH_3OH-H_2O and $C_2H_5OH-H_2O$) with Varying Concentrations[a]

concentration	CH_3OH					C_2H_5OH				
wt %	0	20.9	44.2	70.4	100	0	20.8	44.1	70.3	100
mol %	0	12.9	30.8	57.2	100	0	9.3	23.6	48.1	100
arc stability	B	B	B	B	A	B	B	B	A	A
residual liquid color	X	X	X	X	X	X	light yellow	yellow	light brown	brown
integrated UV−vis spectra (nm)	0	0.6	1.5	11.6	41.3	0	0.2	0.3	1.6	36.9

[a] A = very stable, B = stable, and X = colorless.

TABLE 2: Arc Stability and Color of Residual Liquid after Arc Discharge in Alcohol and Alkane with Varying Carbon Number in Their Molecules[a]

substances	alcohol								alkane	
no. of carbon atoms in molecule	1	2	3	4	5	6	7	8	6	7
arc plasma	A	A	A	A	A	A	A	A	A	A
residual liquid color	X	light yellow	yellow	dark yellow	light orange	orange	black	orange	yellow	dark yellow

[a] Symbols in this table are the same as in Table 1.

After the arc discharge was terminated, three types of products were collected: (1) deposit at the cathode end, (2) fine particles at the vessel bottom, and (3) deposit at the anode end. These products were observed by transmission electron microscopy (TEM) (JEOL, JEM2010), field emission scanning electron microscopy (FESEM) (HITACHI, S-900), and Raman spectroscopy (JASCO, NR1100). Dynamic light scattering (DLS) (MALVERN ZETASIZER300HSA) was chosen for analysis of the particle size distribution. Before the DLS analysis, CNPs were dispersed in toluene by ultrasonification (150 W) for 1−2 min. A dual-beam ultraviolet−visible light (UV−vis) absorption spectrometer (Shimadzu, UV-1600 PC) was used for qualitative analysis on the liquid byproducts. In addition, an optical emission spectrometer (Ocean Optics, OOIBase32) was used for analysis of the arc plasma to estimate its temperature and to observe the carbon cluster formation.

Results and Discussion

Observation of Arc Plasma in Organic Liquids. Plasma Stability and Active Species in Reaction Field. The arc stability in the mixed liquids of CH_3OH-H_2O and $C_2H_5OH-H_2O$ is summarized in Table 1. Here, very stable is defined by the condition in which the brightness of the plasma is continuously stable and the fluctuation of voltage is within 1.5 V. Stable means the situation in which the fluctuation of voltage is within 5 V. With an increasing CH_3OH concentration, the arc plasma tends to become more stable. Also, in the case of the $C_2H_5OH-H_2O$ mixture, the arc plasma becomes more stable with an increasing concentration of C_2H_5OH. Table 2 shows the arc stability in eight kinds of alcohols and two kinds of alkanes in the same manner. As a result, the arc plasma in such organic liquids was very stable. These results indicate that the increase of the carbon concentration in the plasma zone tends to enhance the stability of the arc plasma.

To obtain information on the active species in the arc plasma and its temperature, optical emission spectra from the arc spot in the liquid media were obtained. The typical spectra from water, *n*-alkane (C_7H_{17}), alcohol (C_2H_5OH), and the aromatic compound ($C_6H_5CH_3$) are shown in Figure 1. It can be recognized that there are peaks associated with C_2 at 516 nm and with Hα at 660 nm for every liquid. Hγ at 433 nm was recognized for water, additionally.

To estimate the temperature of the arc plasma, it is common to compare the intensities of two peaks from a species at different excitation states, such as Hγ and Hα. However, these peaks could barely be observed in some liquids. Thus, we

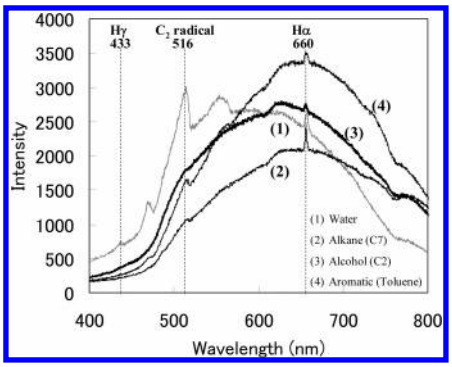

Figure 1. Optical spectra of arc plasma in H_2O, alkanes (C_mH_{2m+2}, $m = 7$), alcohols ($C_mH_{2m+1}OH$, $m = 2$), and aromatic compounds ($C_6H_6-C_nH_{2n+1}$, $n = 1$).

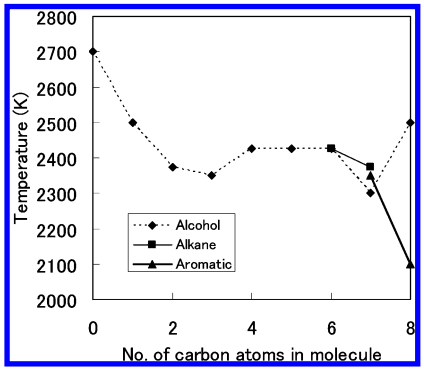

Figure 2. Temperature at the arc plasma in H_2O, alkanes (C_mH_{2m+2}, $m = 6-7$), alcohols ($C_mH_{2m+1}OH$, $m = 1-8$), and aromatic compounds ($C_6H_6-C_nH_{2n+1}$, $n = 1-2$) estimated by Planck's equation.

applied Planck's equation of blackbody radiation for fitting with the spectra curves to estimate the mean temperature of the arc hot zone. This equation is described as eq 1.

$$B_\nu(T) = \frac{2hc^2\nu^3}{\exp(hc\nu/kT) - 1} \quad (1)$$

$B_\nu(T)$, h, c, ν, k, and T are, respectively, the intensity of blackbody radiation as a function of temperature, Planck's constant, light speed, frequency of light, Boltzman's constant, and temperature. The arc temperature estimated for the liquids used in this study is shown in Figure 2. The arc in water induced the highest temperature, and the arc in CH_3OH exhibited the second highest. The temperature of the arc in other alcohols was in the range of 2100−2500 K. At the same carbon numbers

TABLE 3: Heat Balance in Arc in Alcohol System

	carbon number	arc power input E1 (J/s)	specific heat for temperature elevation E2 (J/s)	heat of evaporation E3 (J/s)	E1 − E2 − E3 (J/s)
water	0	764.2	305.4	199.4	259
methanol	1	764.2	105.4	557.9	101
ethanol	2	764.2	171.5	409.6	183
propanol	3	764.2	184.4	332.3	248
butanol	4	764.2	240.2	235.9	288
pentanol	5	764.2	263.1	151.0	350
hexanol	6	764.2	304.1	91.2	369
heptanol	7	764.2	438.3	37.5	288

in the molecules, the arc in alcohols and alkanes exerted almost the same temperature. The arc in aromatic liquids, $C_6H_5CH_3$ and $C_6H_5C_2H_5$, provided a relatively low arc temperature, and $C_6H_5C_2H_5$ showed the lowest temperature.

Energy Balance in Arc-in-Liquid. The energy balance was calculated with consideration about the energy of the arc plasma, the volumetric loss of the liquids, the temperature elevation of the liquids, and conversion of the liquids to solid products. The energy of the arc plasma was obtained from multiplying the arc current by the voltage between the electrodes. We calculated the heat of evaporation with an assumption that the volumetric loss of the liquids was caused by evaporation. In fact, the mass of the solid products was significantly smaller than the mass of the organic liquids lost by the arcing process in all conditions. Thus, we consider this assumption to be a reasonable approximation. The heat for the temperature elevation of the liquid was calculated using the specific heat capacity estimated by the Antoine equation. Table 3 shows the estimated value of energy input of arc plasma E1, the energy to raise the liquid temperature E2, and the energy to evaporate the liquid E3. The value of (E1 − E2 − E3) indicates the upper limit of the energy required to convert the electrode and liquid to the solid products. In the alcohol cases, one can notice that (E1 − E2 − E3) increases with the number of carbons in the alcohol molecules (except $n = 7$). This result indicates that the energetic efficiency to produce solid products would increase when higher alcohol is used.

Characteristics of Product Formation and Structures. Influence of Molar Ratio in $C_2H_5OH-H_2O$ and CH_3OH-H_2O Mixtures. In this work, the arc plasma was generated in a $C_2H_5OH-H_2O$ mixture with a varied C_2H_5OH molar concentration of 9.3, 23.6, 48.1, and 100 mol %. Microscopic analyses revealed that with any concentration of C_2H_5OH, the deposit formed at the cathode tip contained the mixed CNPs, which consisted of MW-CNTs with diameters of 10−30 nm and lengths of 70−400 nm and multi-shelled carbon nanoparticles with diameters of 20−50 nm. Figure 3 shows the typical microscopic images of the synthesized products. These views were seen everywhere by scanning observations, indicating that the purity of CNPs is fairly high. It was impressed that the concentration of CNPs appeared to be approximately 65−70%.

In the products collected from the vessel bottom, CNPs with an extremely low concentration was observed in the pure C_2H_5OH case. However, the concentration of CNPs increases to 40−50% when the C_2H_5OH concentration is decreased to 9−10 mol %. Finally, under the condition of arc-in-water (0 mol % of C_2H_5OH), the concentration of CNPs in the bottom products increased to approximately 50%, which was consistent with other previous work.[13,22] For the deposit formed at the anode end, CNPs were not found, but all obtained structures from the arc-in-$C_2H_5OH-H_2O$ seemed to be graphite and amorphous carbon.

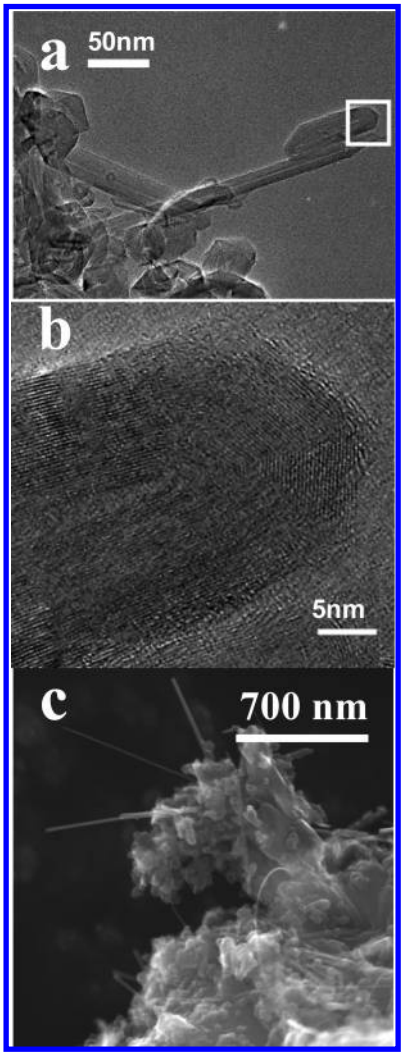

Figure 3. Microscope analyses of the products: (a) TEM image of cathode deposit obtained by arc in pure C_2H_5OH, (b) high-magnification image of the part inside the square in panel a, and (c) FESEM image of cathode deposit obtained by arc in pure CH_3OH.

The production rates and yield of the obtained products that were determined by elaborate weighting are shown in Figure 4a with respect to C_2H_5OH concentration. The production rate of the cathode deposit slightly decreases as the concentration of C_2H_5OH is increased within a low concentration range (<10 mol %). Above this concentration, this production rate increases with the C_2H_5OH concentration up to 3.5 g/h at 100 mol % of C_2H_5OH, which is approximately 4.5 times higher than that in water. The increase in the production rate by use of C_2H_5OH is attributable to the increased carbon vapor content in the gas bubbles emerging from the arc zone. When pure C_2H_5OH is used, 4.17×10^{19} atoms/m^3 of carbon is supposed to exist in

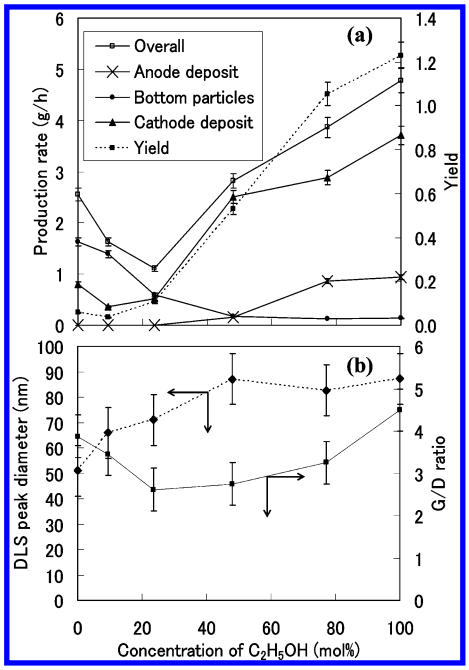

Figure 4. Influence of the concentration of C_2H_5OH on (a) production rate and yield of obtained products and (b) DLS peak diameter and G/D ratio of CNPs in the cathode deposit.

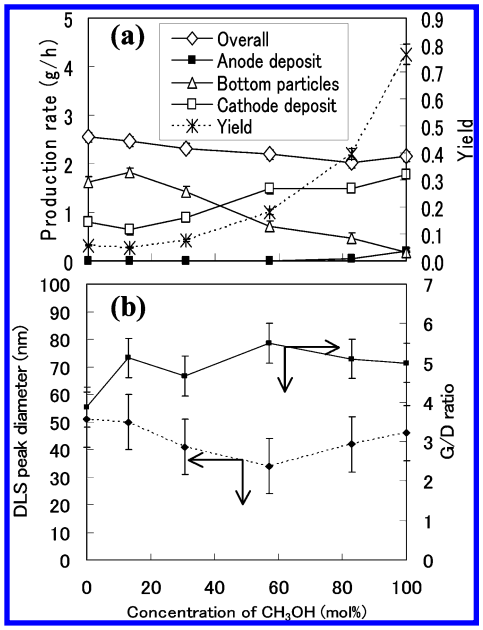

Figure 5. Influence of the concentration of CH_3OH on (a) production rate and yield of obtained products and (b) DLS peak diameter and G/D ratio of CNPs in the cathode deposit.

the bubbles, assuming that C_2H_5OH vapor is generated by boiling at atmospheric pressure at the arc zone. It should be noted that the production rate of the bottom products decreases while the other production rates increase with the increasing concentration of C_2H_5OH. The reason for this result has not yet been clarified. Nevertheless, this result may be associated with the influence of the quenching rate of carbon vapor. One may consider that the quenching rate in C_2H_5OH may be higher than that in H_2O at a constant arc temperature because of its higher heat capacity.[28] However, this relation may be reversed because the arc temperature in C_2H_5OH is much lower than that in water as shown in Figure 2.

The yield of the CNP-rich cathode deposit was determined by the ratio of the weight of cathode deposit to that of the consumed anode. When this value is higher than unity, it suggests that the carbon source for CNPs formation is not only the graphite electrode but also the liquid. It can be clearly seen in Figure 4a that in the case of pure C_2H_5OH, the yield reaches 1.23. This result implies that C_2H_5OH plays a role in the carbon source for the production of CNPs. On the contrary, in the arc-in-water system, carbon atoms were only supplied from the graphite electrodes, leading to a very low yield of approximately 0.1. It is noteworthy that the yield of the CNP-rich cathode deposit from pure C_2H_5OH is about 12 times higher than that of the conventional arc-in-water condition. This result suggests that the carbon source in the arc-in-C_2H_5OH condition is mainly C_2H_5OH.

The peak diameter of the CNP-rich products estimated by DLS is shown in Figure 4b. It is obvious that the mean hydrodynamic diameter of CNPs in every case ranges 40−100 nm. The mean diameter slightly increases with the increasing concentration of C_2H_5OH. This result implies that there are more elongated structures in CNPs generated by arc-in-C_2H_5OH. Orlanducci et al. have reported that the formation of the elongated particles such as MW-CNTs needs more carbon supply than that of short-shaped CNPs.[29] Therefore, the result shown here should be attributed to the higher concentration of carbon vapor generated in C_2H_5OH than that in H_2O.

The ratio of the intensity of the graphitic band (G-band, 1580 cm^{-1}) to that of the disorder band (D-band, 1353 cm^{-1}) in the Raman spectra of CNP-containing deposits is also shown in Figure 4b. With varying the concentration of C_2H_5OH, the G/D ratio varies in the range of 2.7−4.5. The G/D ratio becomes the lowest at 30 mol % of C_2H_5OH and turned to a maximal value when pure C_2H_5OH was used. It can be expected that in the range of a relatively low C_2H_5OH concentration, the oxidative species induced from H_2O could react with carbon to terminate the growth of CNPs, resulting in their structural defects. In a high C_2H_5OH concentration range, a high concentration of carbon in the arc plasma zone could support continuous growth of CNPs, leading to the improvement of the crystallinity of the products and the G/D ratio.

Meanwhile, the arc-in-CH_3OH-H_2O mixture was also investigated in a manner similar to the $C_2H_5OH-H_2O$ case. The concentration of CH_3OH was varied in a range of 12.9, 30.8, 57.2, and 100 mol %. A typical FESEM image of products synthesized by arc-in-CH_3OH-H_2O is shown in Figure 3c. It was found that CNPs existed not only in the cathode deposit but also in the powdery deposit at the reactor bottom in all conditions, although the concentration of CNPs in the cathode deposit is higher than that in the bottom products. On the other hand, the anode deposit obtained in the CH_3OH-H_2O system mainly consisted of graphite and amorphous particles without the CNPs similar to the products of the $C_2H_5OH-H_2O$ case.

Figure 5a shows the production rates of the products synthesized in the CH_3OH-H_2O mixture. The formation rate of the cathode deposit slightly decreased as the concentration of CH_3OH was increased up to 10−15 mol %. Above this concentration, the production rate of the CNP-rich cathode deposit significantly increased with increasing CH_3OH concentration, while the formation rate of the bottom products oppositely decreased. Consequently, the overall production rate slightly decreased as the concentration of CH_3OH was increased. Meanwhile, the yield of the CNP-rich cathode deposit became higher with an increasing concentration of CH_3OH. The highest yield of 0.76 was obtained when pure CH_3OH was used. Similarly to the case of $C_2H_5OH-H_2O$, the higher concentration

of carbon vapor in the emerging bubbles can be expected when the higher CH_3OH concentration in the liquid media is employed.

DLS analysis of the CNP contained cathode deposit formed at each CH_3OH concentration is also shown in Figure 5b. This figure reveals that the mean hydrodynamic diameter of the CNPs synthesized by arc-in-CH_3OH-H_2O is in a range of 25−60 nm. In the conditions above 60 mol % of CH_3OH, similar to the $C_2H_5OH-H_2O$ system, the ascending carbon vapor concentration at the arc zone accounted for the enhancement in the growth of the elongated particles, leading to the increase of mean diameter of CNPs with a higher CH_3OH concentration. In the conditions below 60 mol % of CH_3OH, the mean diameter of CNPs decreased with the CH_3OH concentration. Although the reason for this result has not yet been clarified, we consider that this trend may be caused by the decrease of the arc temperature.

In a comparison between Figure 4b and Figure 5b, it is seen that the G/D ratio of the Raman spectra is less sensitive to the concentration of CH_3OH as compared with the case of C_2H_5OH. This result is attributed to the lower number of carbon atoms in the CH_3OH molecule, resulting in less additional carbon atoms supplied to the self-assembling reaction of CNPs.

Influence of Number of C Atoms in *n*-Alcohol ($C_mH_{2m+1}OH$, $m = 1-8$). The *n*-alcohols of various molecular weights ($C_mH_{2m+1}OH$, $m = 1-8$) were used for the liquid media accommodating the arc plasma to synthesize CNPs. Microscope analyses by FESEM and TEM suggested that cathode deposits contained CNPs consisting of MW-CNTs and multi-shelled nanoparticles of high concentrations. The MW-CNTs have a diameter of 10−20 nm and a length of 400 nm to more than 1 μm, while the multi-shelled nanoparticles have a diameter of about 20−70 nm. On the other hand, the synthesized products settling down at the vessel bottom contained mainly graphite and amorphous carbon. The concentration of CNPs mixed in such products was remarkably lower than that in the cathode deposit. Meanwhile, the structure of synthesized product depositing on the anode was similar to those in the cases of the CH_3OH-H_2O and $C_2H_5OH-H_2O$ mixtures, in which the CNPs were rarely observed.

The production rates of the products shown in Figure 6a suggest that when the number of carbon atoms (m) in the alcohol molecule is increased, the overall production rate and the production rate of the cathode deposit become higher with m up to 6. With *n*-heptanol or *n*-octanol, the production rate becomes gradually decreased with m. The sediment products found at the vessel bottom slightly increase with the increasing carbon number in the alcohol. The relationship between the yield of the CNP-rich cathode deposit and the number of carbons in the alcohol is also shown in Figure 6b. The yield tends to increase with the carbon number and reaches the highest value of approximately 10.0 when *n*-heptanol ($m = 7$) is employed. Interestingly, this value is about 100 times as that in the conventional arc-in-water condition. This result suggests that the main carbon source in the arc-in-alcohol should be the alcohol but not the graphite electrodes.

As shown in Figure 7a, the particle size analysis by DLS reveals that the mean hydrodynamic diameter ranges from 40 to110 nm in every case of arc-in-alcohol. The mean particle diameter in all of the alcohols except methanol is larger than that of the arc-in-water system. This result implies that the relatively high concentration of carbon atoms in the reaction field gives rise to the preferable growth of elongated products. Therefore, the selectivity of MW-CNTs to multi-shelled nanoparticles in alcohols should become higher than that in the arc-in-water condition, which is consistent with microscopy analyses.

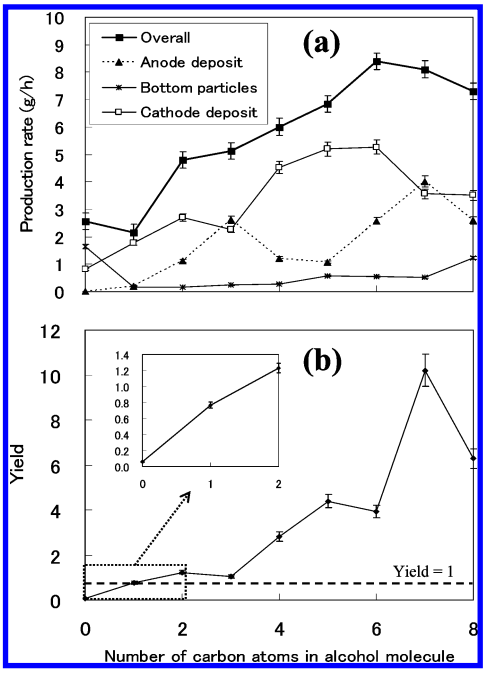

Figure 6. Influence of the number of carbon atoms in alcohol molecules on (a) production rate of obtained products and and (b) the yield of CNP-rich product.

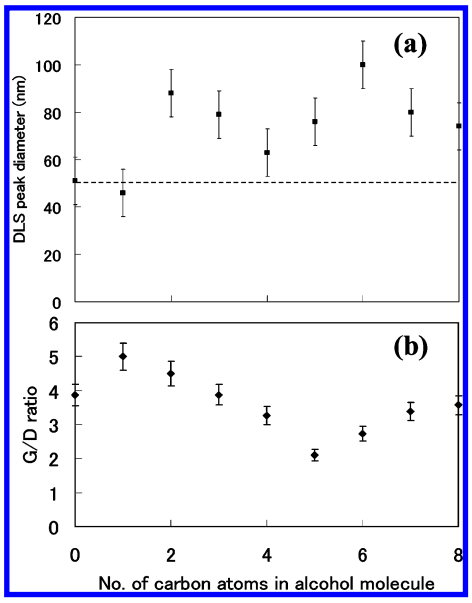

Figure 7. Influence of the number of carbon atoms in alcohol molecules on (a) DLS peak diameter of CNP-rich product and (b) G/D ratio of CNPs-rich product in Raman analyses.

The G/D ratio in the Raman spectra of the CNP-rich product synthesized in alcohols is shown in Figure 7b. When the alcohol with a longer chain was employed, the G/D ratio decreased continuously up to $m = 5$. The reason for the appearance of this minimum peak is not clarified. Nevertheless, we consider that the decrease of the G/D ratio with the carbon number in alcohol molecules in the low carbon number range is related to the arc temperature as shown in Figure 2. Namely, the lower temperature may cause the lower G/D ratio. When the C number comes to more than 5, the increase of the carbon concentration in the plasma region may enhance the crystallinity of the products, while the arc temperature does not significantly

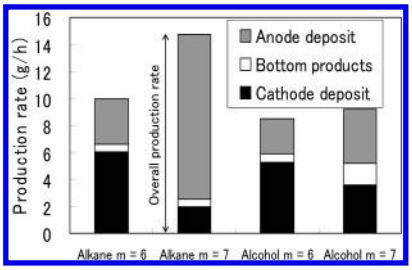

Figure 8. Influence of the number of carbon atoms in alkane molecules on the production rate of obtained products as compared with alcohol cases.

decrease with the C number in this range. Also, one may consider that the decrease of the G/D ratio with respect to the carbon number in alcohol may be attributed to the excess energy, which is related with the heat balance summarized in Table 3. Here, (E1 − E2 − E3) exerts an optimum when *n*-pentanol or *n*-hexanol is employed. This energy contains the energy for the CNP formation and the excess energy to form impurities. This excess energy could result in excess carbon atoms, which would preferably undergo amorphous phase formation.[30]

Influence of Number of C Atoms in *n*-Alkanes (C_mH_{2m+2}, $m = 6-7$). Two *n*-alkanes, haxane and heptane, were selected because their physical properties (vapor pressure, etc.) were appropriate for accommodating the arc. Microscopic analyses using FESEM revealed that the cathode deposit formed by the arc-in-alkane contained the CNPs that consisted of MW-CNTs and multi-shelled nanoparticles similar to the products of arc in alcohols. Also, the other products collected from the vessel bottom and at the anode tip were graphite and disordered carbon with a very low concentration of CNPs.

The production rates of the synthesized products are shown in Figure 8. It is seen that the overall production rate in alkanes is higher than that in alcohol with the same carbon number. Meanwhile, the production yield of the cathode deposit based on the consumed anode was obtained from the arc-in-hexane and arc-in-heptane as 2.7 and 1.3, respectively. It should be mentioned that the selectivity of the CNP-rich cathode deposit obtained from these alkanes was lower than that from alcohols.

It is notable that the heat of evaporation of hexane and heptane is lower than those of hexanol and heptanol, respectively.[28] Therefore, the formation of alkane vapor during arc is supposedly higher than that of alcohols. However, the existence of oxygen in the alcohol molecules would oppositely result in oxidation to remove amorphous carbon, which is less stable than crystalline carbon.[32] These competitive effects may cause the increase of the production rate and the decrease of the selectivity of CNPs synthesized by arc in alkanes as compared with that by arc in alcohols. The lower selectivity of CNPs synthesized in alkanes could be confirmed by the ratio of the G/D peak obtained from the Raman spectroscopic analyses.

On the basis of the DLS analyses, the particle size distribution of the CNP-rich product obtained from arc-in-alkanes exhibited mean hydrodynamic diameters of 70 and 68 nm for hexane and heptane, respectively. It should be noted that arc-in-water could give rise to the synthesized product with the mean hydrodynamic diameter of 51 nm (also shown as a threshold in Figure 7a). Therefore, it may be implied that the existence of extra carbon atoms in the arc zone in the alkane liquid also could provide preferable conditions for the growth of elongated CNPs as compared with that in water.

Case of Aromatic Liquid ($C_6H_6-C_nH_{2n}$, $n = 1,2$). Two aromatic compounds, toluene and ethyl benzene, were employed to accommodate the arc plasma that provided three types of products similar to those of arc-in-alcohols and -alkanes. However, the anode deposit formed in the aromatic liquids exhibited a distinct shape, which was a skirt-like shape, as shown in Figure 9. This skirt-like anode deposit was also observed in a previous investigation of arc-in-benzene.[27] Although certain amounts of MW-CNTs and multi-shelled nanoparticles were observed in the cathode deposit by TEM, disordered carbon was the main product of arc in both toluene and ethyl benzene. In the settling products and anode deposit, only graphite and disordered carbon without CNPs were found.

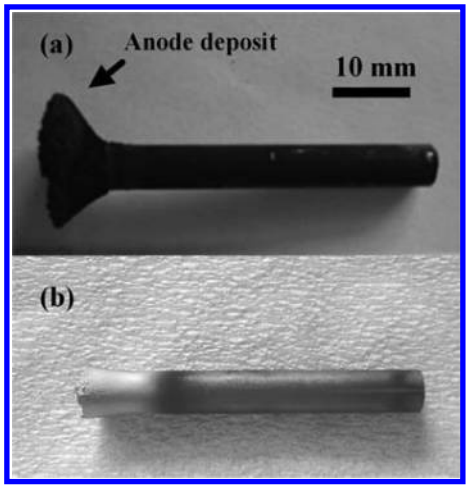

Figure 9. Photograph of the anode rod after arc in (a) $C_6H_5CH_3$ and in (b) C_2H_5OH.

TABLE 4: Types of Obtained Products by Arc in Organic Compounds[a]

			aromatic compounds		
type of products	alcohol	alkane	benzene	toluene	ethylbenzene
cathode deposit	ABC	ABC	BC[b]	ABC	ABC
bottom particles	BC	BC	C	C	C
anode deposit	C	C	C	C	C

[a] A = MW − CNTs; B = multi-shelled nanoparticles; and C = other carbon structures (graphite, amorphous, and disordered carbons). [b] No CNTs were found.

For comparison, the structures of the products synthesized by arc-in-organic compounds investigated in the present work and the previous work on arc-in-benzene[27] are summarized in Table 4. In the settling products (bottom particles), only multi-shelled nanoparticles with extremely low concentrations of MW-CNTs were obtained from arc-in-alcohols and -alkanes. Meanwhile, substantial amounts of MW-CNTs and multi-shelled nanoparticles were found in the cathode deposit of arc-in-alcohols and -alkanes, but the concentration of CNPs became much lower when aromatic compounds were used. These results mean that the alkyl groups play an important role in the carbon source to synthesize CNPs, while the aromatic group should inhibit the formation of crystalline CNPs.

Characteristics of Residual Liquids. There are several articles about organic byproducts generated by arcing in some liquids.[23−26,33] In the present work, the color of the liquid changed remarkably during the arcing process in many conditions as summarized in Tables 1 and 2. Furthermore, UV−vis absorption analyses of the residual liquids obtained from the arc-in-alcohols, -alkanes, and -aromatics are shown in Figures 11 and 12. Although the residual liquid obtained from arc-in-CH_3OH and mixtures of H_2O and CH_3OH was visually colorless, the UV−vis absorption spectra obviously exhibited the absorbance in the UV region (with a wavelength shorter than 300 nm). This means that some colorless byproducts were

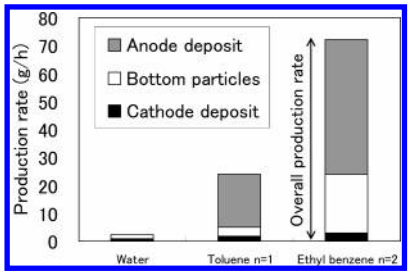

Figure 10. Influence of the species of aromatic compounds on production rate of obtained products as compared with water.

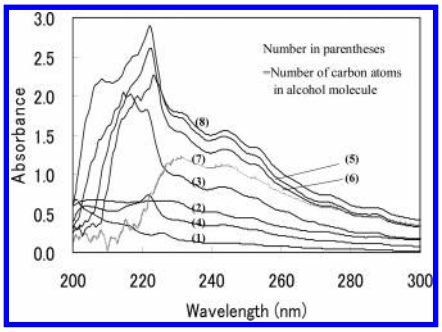

Figure 11. UV−vis absorbance spectra of residual liquid after arc in alcohols.

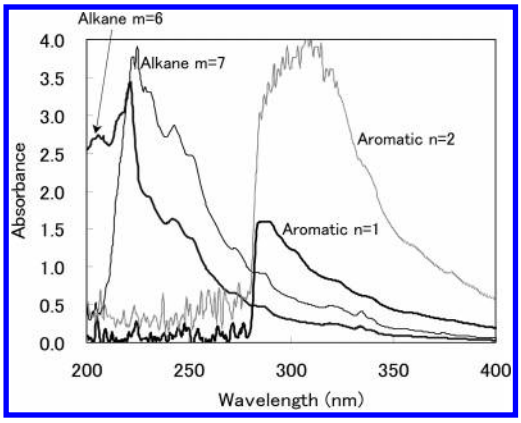

Figure 12. UV−vis absorbance spectra of residual liquid after arc in alkanes and aromatics.

generated. The concentration of such byproducts could be qualitatively evaluated by integrating the area under the UV spectra as summarized in Table 1. It is notable that the production rates of the byproducts increase with the increasing concentration of these alcohols in their aqueous mixtures.

The colors of residual liquids from the arc-in-pure alcohols are summarized in Table 2. According to the analyses of the UV−vis absorbance spectra of these liquids shown in Figure 11, the components and the quantities of the byproducts are dependent on the number of carbon atoms in the alcohol molecules. It is reasonable that the quantities and variations of the byproducts would tend to increase with the increasing carbon atoms in the molecules of the liquids.

The color of the residual liquids obtained from arc-in-alkanes is lighter than that of arc-in-alcohols as shown in Table 2. In the UV−vis absorbance spectra of the residual liquids from the arc-in-hexane and -heptane shown in Figure 12, the spectral peaks in the range of 210−250 nm can be seen similarly to that of arc-in-alcohols. This result suggests that the byproducts formed by arc-in-alkanes contain molecular structures similar to those formed by arc-in-alcohols.

The colors of the residual liquids remaining after the arc-in-toluene and -ethyl benzene were different from those observed in the arc-in-alcohols and -alkanes. Their colors were red and brown, respectively. In the UV−vis analyses, shown in Figure 12, the residual liquids obtained from arc-in-toluene and -ethyl benzene commonly exhibited the spectral peaks in a range higher than 270 nm, which are significantly different from those of arc-in-alcohols and -alkanes. From the feature of the UV−vis spectra, the molecular structure of the byproducts formed in the aromatics should be substantially different from those in alcohols and alkanes.

Further analyses to identify the liquid byproducts are currently underway because the analyses on the components of the liquid byproducts are crucial to understanding the reaction mechanisms. There are some previous papers related with this work. Beck et al. reported mass spectrometric analyses of many kinds of polycyclic aromatic hydrocarbons (more than 60 compounds), which were generated by arc discharge in toluene.[33] In addition, Cataldo recently reported H-terminated polyynes generated by arc-in-methanol and -hexane.[23−25]

Conclusion

Organic compounds that are alcohols ($C_mH_{2m+1}OH$, $m = 1-8$), alkanes (C_mH_{2m+2}, $m = 6-7$), and aromatics ($C_6H_6-C_nH_{2n}$, $n = 1-2$) were used as liquid media to accommodate the arc plasma between graphite electrodes to synthesize CNPs, which included MW-CNTs and multi-shelled carbon nanoparticles. The CNPs with relatively high concentrations were selectively found in the hard deposits at the cathode tip when the alcohols and alkanes were employed. Meanwhile, arc-in-aromatic compounds did not provide preferable quantity of CNPs as compared with those of arc-in-alcohols and -alkanes. The present work revealed that organic compounds play a crucial role as a carbon source to generate CNPs, resulting in approximately an 8−100 times higher yield of CNP-rich product when compared with that of conventional arc-in-water. Larger hydrodynamic diameters of CNPs were observed when the number of carbon atoms in molecule of the accommodating liquid was increased. The mechanism of the effect of the liquid components on the yield and the structures of the products were discussed with consideration of the arc temperature and heat balance in the relevant arcing system. Finally, the generation of organic byproducts during the arc discharge exhibited the dependence based on the types of the initial organic liquids.

Acknowledgment. The authors acknowledge financial support from Research Team Award of Thailand Research Fund (RTA-TRF for W.T.); the University-Industry collaborative project of CU; AIEJ Scholarship; Thailand−Japan Technology Transfer Project (TJTTP-OECF) of CU; and a Grant-in-Aid for Young Scientists (A) of the Japan Society for the Promotion of Science (JSPS).

References and Notes

(1) Kroto, H. W.; Heath, J. R.; O'Brien, S. C.; Curl, R. F.; Smally, R. E. *Nature* **1985**, *318*, 162.

(2) Iijima, S. *Nature* **1991**, *354*, 56.

(3) Iijima, S.; Ichihashi, T. *Nature* **1993**, *363*, 603.

(4) Iijima, S.; Yudasaka, M.; Yamada, R.; Bandow, S.; Suenaga, K.; Kokai, F.; Takahashi, K. *Chem. Phys. Lett.* **1999**, *309*, 165.

(5) Ugarte, D. *Nature* **1992**, *359*, 707.

(6) Ruoff, R. S.; Lorents, D. C.; Chan, B.; Malhotra, R.; Subramoney, S. *Science* **1993**, *259*, 346.

(7) Thess, A.; Lee, R.; Nikolaev, P.; Dai, H.; Petit, P.; Robert, J.; Xu, C.; Lee, Y. H.; Kim, S. G.; Colbert, D. T.; Scuseria, G.; Tománek, D.; Fischer, J. E.; Smalley, R. E. *Science* **1996**, *273*, 483.

(8) Endo, M.; Takeuchi, T.; Igarashi, S.; Kobori, K.; Shiraishi, M.; Kroto, H. W. *J. Phys. Chem. Solids* **1993**, *54*, 1841.

(9) Nozaki, T.; Kimura, Y.; Okazaki, K. *J Phys. D: Appl Phys.* **2002**, *35*, 2779.
(10) Ebbesen, T. W.; Ajayan, P. M. *Nature* **1992**, *358*, 220.
(11) Kato, T.; Jeong, G.-H.; Hirata, T.; Hatakeyama, R.; Tohji, K.; Motomiya, K. *Chem. Phys. Lett*. **2003**, *381*, 422.
(12) Chhowalla, M.; Teo, K. B. K.; Ducati, C.; Rupesinghe, N. L.; Amaratunga, G. A. J.; Ferrari, A. C.; Roy, D.; Robertson, J.; Miline, W. I. *J. Appl. Phys*. **2001**, *90*, 5308.
(13) Sano, N.; Wang, H.; Chhowalla, M.; Alexandrou, I.; Amaratunga, G. A. J. *Nature* **2001**, *414*, 506.
(14) Sano, N.; Wang, H.; Alexandrou, I.; Chhowalla, M.; Teo, K. B. K.; Amaratunga, G. A. J. *J. Appl. Phys.* **2002**, *92*, 2783.
(15) Sano, N.; Naito, M.; Chhowalla, M.; Kikuchi, T.; Matsuda, S.; Iimura, K.; Wang, H.; Kanki, T.; Amaratunga, G. A. J. *Chem. Phys. Lett.* **2003**, *378*, 29.
(16) Hsin, Y. L.; Hwang, K. C.; Chen, F. R.; Kai, J. J. *Adv. Mater.* **2001**, *13*, 830.
(17) Zhu, H. W.; Li, X. S.; Jiang, B.; Xu, C. L.; Zhu, Y. F.; Wu, D. H.; Chen, X. H. *Chem. Phys. Lett*. **2002**, *366*, 664.
(18) Cadek, M.; Murphy, R.; McCarthy, B.; Drury, A.; Lahr, B.; Barklie, R. C.; Panhuis, M.; Coleman, J. N.; Blau, W. J. *Carbon* **2002**, *40*, 923.
(19) Antisari, M. V.; Marazzi, R.; Krsmanovic, R. *Carbon* **2003**, *41*, 2393.
(20) Lange, H.; Sioda, M.; Huczko, A.; Zhu, Y. Q.; Kroto, H. W.; Walton, D. R. M. *Carbon* **2003**, *41*, 1617.
(21) Biro, L. P.; Horvath, Z. E.; Szalmas, L.; Kertesz, K.; Weber, F.; Juhas, G.; Radnoczi, G.; Gyulai, J. *Chem. Phys. Lett.* **2003**, *372*, 399.
(22) Sano, N.; Charinpanitkul, T.; Kanki, T.; Tanthapanichakoon, W. *J. Appl. Phys.* **2004**, *96*, 645.
(23) Cataldo, F. *Carbon* **2004**, *42*, 129.
(24) Cataldo, F. *Tetrahedral Lett.* **2004**, *45*, 141.
(25) Cataldo, F. *Tetrahedron* **2004**, *60*, 4265.
(26) Cataldo, F. *Polyhedron* **2004**, *23*, 1889.
(27) Sano, N. *Mater. Chem. Phys*. **2004**, *88*, 235.
(28) Dean, J. A. *Lange's handbook of chemistry*, 3rd ed.; McGraw-Hill: New York, 1985.
(29) Orlanducci, S.; Valentini, F.; Piccirillo, S.; Terranova, M. L.; Botti, S.; Ciardi, R.; Rossi, M.; Palleschi, G. *Mater. Chem. Phys*. **2004**, *87*, 190.
(30) Zhao, X. L.; Ohkohchi, M.; Inoue, S.; Suzuki, T.; Kadoya, T.; Ando, Y. *Diamond Relat. Mater.*, in press.
(31) Akita, S.; Ashihara, H.; Nakayama, Y. *Jpn. J. Appl. Phys*. **2000**, *39*, 4939.
(32) Maruyama, S.; Kojima, R.; Miyauchi, Y.; Chiashi, S.; Kohno, M. *Chem. Phys. Lett.* **2002**, *360*, 229.
(33) Beck, M. T.; Dinya, Z.; Keki, S. *Tetrahedron* **1992**, *48*, 4919.